

Rigidity transition in two-dimensional random fiber networks

M. Latva-Kokko, J. Mäkinen, and J. Timonen

Department of Physics, University of Jyväskylä, P.O. Box 35 FIN-40351 Jyväskylä, Finland

(Received 10 July 2000; published 28 March 2001)

Rigidity percolation is analyzed in two-dimensional random fibrous networks. The model consists of central forces between the adjacent crossing points of the fibers. Two strategies are used to incorporate rigidity: adding extra constraints between second-nearest crossing points with a probability p_{sn} , and “welding” individual crossing points by adding there four additional constraints with a probability p_{weld} , and thus fixing the angles between the fibers. These additional constraints will make the model rigid at a critical probability $p_{sn} = p_c^{sn}$ and $p_{weld} = p_c^{weld}$, respectively. Accurate estimates are given for the transition thresholds and for some of the associated critical exponents. The transition is found in both cases to be in the same universality class as that of the two-dimensional central-force rigidity percolation in diluted lattices.

DOI: 10.1103/PhysRevE.63.046113

PACS number(s): 64.60.Ak

I. INTRODUCTION

Scalar percolation [1] is a simple model describing the transfer of a scalar conserved quantity, e.g., an electric charge across a randomly diluted system. In two dimensions the geometric exponents of connectivity percolation are known exactly [1,2]. Elastic percolation is not, in general, equivalent to scalar percolation. This was first discovered by Feng and Sen [3]. Since then, considerable attention has been given to the classification of rigidity transition in elastic systems. If angular forces are present, only singly connected paths are required for rigidity and hence the geometric properties of the elastic backbone are exactly the same as those of the scalar percolation problem [4,5]. In central force systems [3,6–21], the singly connected paths are not enough to ensure rigidity. For a long time the only approach used in this problem was to directly solve the elastic equations [6–9,22–24]. The concepts of rigidity percolation such as zero-energy motion (or floppy modes) and constraint counting, have been used for disordered materials such as glasses [25–29]. Recently, numerical algorithms (matching algorithms) [11–16] based on graph theory have made larger system sizes available for simulation. The use of these algorithms has given a new insight into the nature of the rigidity transition. Rigidity percolation has been studied with matching algorithms in diluted lattices [12–14,18,30], Cayley trees [18,19,21], aperiodic lattices [20], and random networks [17]. Directed rigidity percolation has also been studied [31]. The objective of this paper is to study the off-lattice rigidity transition in a random network, and to classify in this case the transition.

The two-dimensional random network is a geometrical structure. It can be used, e.g., to model planar structures that are composed of randomly positioned thin linelike objects (e.g., fibers in a sheet of paper). The statistical properties of this kind of two-dimensional (2D) random networks are well known [32]. To understand the multiple connectivity of such a random network, one can calculate [32] properties such as the average number of crossing points per fiber, the number of polygons in a network, and the average number of sides in a polygon. In our model, the 2D fiber network is generated by randomly placing 1D objects of equal length on a plane so that both x and y coordinates and the orientation angles of the

fibers are taken from a uniform distribution. We use periodic boundary conditions in the y direction, and a box of linear size L plus one fiber length in the x direction to minimize the boundary effects, and to keep the fiber density unchanged on the boundaries. Figure 1 shows a typical 2D random network.

A system is rigid if it cannot be deformed without changing its energy, i.e., if any small deformation of the system has a nonzero response. A system is nonrigid or floppy if it can be continuously deformed without change of energy. The number of (linearly) independent motions that do not cost energy is called the number of floppy modes of the system. In a central-force network one can write the energy of the system in the form,

$$E = \frac{1}{2} \sum_{i,j} [(\vec{u}_i - \vec{u}_j) \cdot \vec{R}_{ij}]^2 e_{ij}. \quad (1)$$

For the energy to be minimized, we require $\partial E / \partial u_i = 0$ for $\forall i$, which is necessary for the equilibrium configuration of the network. If one deforms the equilibrium configuration and solves the resulting set of linear equations, the number of

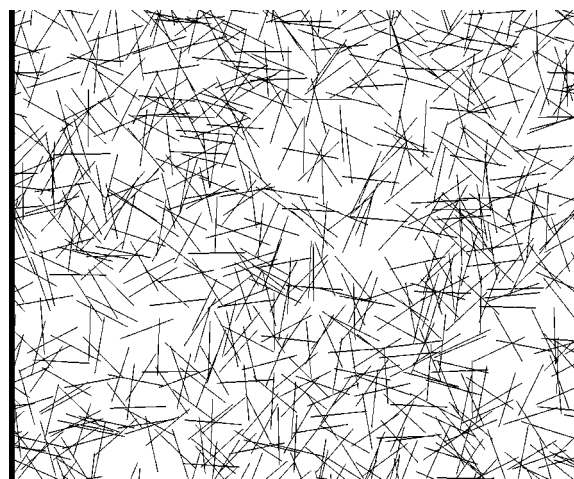


FIG. 1. A typical 2D random network with density $q = 2q_c$ (see text for the definitions of q and q_c).

floppy modes is the number of degrees of freedom minus the number of linearly independent constraints in the system.

Although rigidity and the rigidity transition can, in principle, be studied with dynamical methods, rigidity is a static property. The dynamical methods have proved to be ineffective in rigidity analysis because of the restrictions [6–9,22,23] on the size of the system that can be analyzed. The idea of generic rigidity [12,13] solves some of these problems. In generic rigidity the geometrical singularities, i.e., pathological configurations, are ignored, and constraint counting is used for calculating the degrees of freedom and the number of independent constraints in the system. A random network is inherently generic because the random construction eliminates any possibility for a geometrical singularity, i.e., the probability of geometrical singularities is zero. The simplest argument used [14,33] by Maxwell to check whether a system is rigid was to calculate the number of floppy modes as the difference of the degrees of freedom and the number of constraints (i.e., all constraints are assumed independent). If the number of floppy modes of a d -dimensional system is less than or equal to the number of collective motions of a d -dimensional body, the system is rigid. To map the redundant constraints, one needs to check this property for every subset of the system. This can be done using recursive matching algorithms, one version of which, due to Jacobs and co-workers [12,16], is called the pebble game. This algorithm calculates the number of floppy modes, maps the overconstrained regions, and identifies all rigid clusters in a 2D generic bar-joint network.

We study the rigidity transition in fiber networks using the concepts of generic rigidity. This is done to gain better insight into the statistical properties of the fiber networks that depend upon rigidity. Generic models are used to better estimate the number of floppy modes and the number of overconstraints or the amount of stress bearing parts in such networks. In real systems that can be modeled by random networks, the amount of fibers is huge (at least of the order of 10^9), and the dynamical methods would be impossible to use. The typical applications for these networks include, e.g., the mechanical [17,32] and transport [17] properties of paper sheets. Here we are mainly interested in the amount of stress bearing regions and in the sizes and shapes of these regions especially near the rigidity transition.

II. METHODS

In the analysis of rigidity in 2D random fiber networks, we use here a matching algorithm, more specifically the pebble game by Jacobs and co-workers [12,16]. This algorithm maps the overconstrained areas and determines the number of floppy modes in the system. It basically represents the degrees of freedom in a system with pebbles. Once a degree of freedom is bound, a pebble is bound, and hence one can keep track of the rigidity in a recursive fashion.

The simplest way to realize an elastic random network is to replace each crossing point with a mass point, which has two degrees of freedom in two dimensions, and each nearest neighbor connection with a Hooke spring, i.e., a single constraint. The simplest nontrivial rigid structure is now a tri-

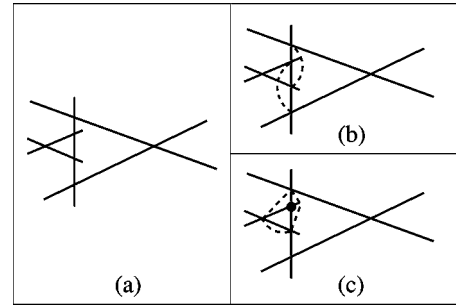


FIG. 2. (a) A structure in the random spring network that should be made rigid. (b) The second-nearest-neighbor strategy in which adding of snn bonds makes the vertical fiber rigid against bending and (c) the welding strategy in which adding of four extra bonds (dashed lines) will make the angles between the crossing fibers stiff.

angle, and a network constructed of triangles would be rigid. Because only two fibers can cross at a single point (the probability of more than two fibers crossing at the same point is negligible), in the network constructed of springs and mass-points, rigidly connected triangles can never percolate and the network will not be rigid at any finite density [17]. More constraints must therefore be introduced in the network in order to make it rigid.

There are several ways by which rigidity can be introduced in a random spring network. Of the possible mechanisms, one should choose those that are relevant for physical applications. It would be desirable, e.g., that the structures such as those in Fig. 2 would be rigid. If the long vertical lines in this figure were rigid, i.e., would not bend without cost of energy, the structure would indeed be rigid. This can be accomplished by adding extra springs along a fiber (line) between second-nearest-neighbor crossing points. An alternative strategy would be to weld crossing points, i.e., to fix the angles between the crossing fibers at some points. The first of these strategies corresponds to a situation in which the fibers become stiff but are still able to orientate freely relative to one another. This happens if cohesion inside (or equivalently on the surface of) the fiber is larger than the forces between the fibers. The welding strategy corresponds to a situation in which two bonded fibers cannot move relative to one another but can still bend. The formation and drying of the paper web in the paper making process is a combination of these two mechanisms but typically the orientational (i.e., welding type) mechanism is dominant. Other random networks could have a stronger tendency for stiffness. The first of these strategies turns out to be easier to implement for large systems. We also get better statistics for this strategy.

We generate a random network by randomly placing N_f fibers of length l in an area of $L \times L$. We use as a control parameter the density of fibers, $q = N_f/L^2$, and denote by q_c the density at the connectivity-percolation threshold. When a random network is generated, we add a simple constraint between each of the nearest neighbors, i.e., replace the fiber segments connecting the crossing points with springs. We first study the rigidity transition in the random spring network of a given density by adding there second-nearest-neighbor constraints with a probability p_{sn} . This will make

the system rigid at a certain probability $p_{sn} = p_{sn}^c$. The transition probability is evaluated by checking the existence of a rigid cluster that would span across the whole network from left to right. This is done using a fictitious bond between the left and right sides of the network and checking its redundancy [15]. As p_{sn} is increased, we monitor the sizes of the rigid clusters and the change in the number of floppy modes. When the transition probability is reached, we check the number of cutting bonds, i.e., the bonds that cannot be removed without loss of the rigid backbone, and the sizes of the isostatic, i.e., minimally rigid regions connected to the backbone.

We also study the rigidity transition in the random spring network using the welding strategy. After generating a nearest-neighbor random network, we add four additional constraints at crossing points with a probability p_{weld} . These constraints will make the system rigid at p_{weld}^c . We evaluate this transition probability p_{weld}^c and monitor the size of the rigid backbone as a function of linear system size L .

We have checked whether the concepts of generic rigidity apply by calculating the number of linearly independent constraints directly from the rigidity matrix. If one does not use additional constraints (i.e., only nearest neighbor bonds) the number of floppy modes as calculated from the rigidity matrix is the same (small deviations are possible by, e.g., 1–5 linearly dependent bonds, but these only constitute at most 0.1% of all bonds) for small systems [(1–5) × $L = 100 - 1500$ crossing points]. For the welding strategy this is also true for welding constraints. This gives us a reason to believe that the concept of generic rigidity is applicable. For the second-nearest-neighbor bonds, we have to assume genericity in the network, i.e., that the crossing points along a fiber cannot lie on the same line or they are linearly dependent. If one assumes genericity and deviates the coordinates even slightly, the rigidity matrix and the pebble game already give the same answers and generic rigidity is applicable. When second nearest neighbors are added in straight fibers, the fibers are left shaky (i.e., they are not first-order rigid). If we accept the idea that the function of snn bonds is to make fibers stiff, we can use in a straightforward fashion generic rigidity.

III. RESULTS

A. Maxwell counting

Once we know the topology, i.e., the connectivity of a random network, we can calculate its number of floppy modes. A surprisingly good estimate for the number of unbound degrees of freedom (floppy modes) is given by the simple constraint counting, Maxwell counting. Maxwell counting neglects the possibility of constraints being dependent, every constraint is assumed to bind one degree of freedom.

If there are n crossing points on a fiber, there are $2n$ degrees of freedom associated with these crossing points. Of these degrees of freedom $n - 1$ are bound since there are $n - 1$ central-force constraints on such a fiber. Each fiber has two end segments. These have four degrees of freedom of

which two are always bound. Finally, every crossing point connects two distinct fibers so the number of unbound degrees of freedom per fiber is

$$\frac{2n}{2} - (n - 1) + 4 - 2 = 3. \quad (2)$$

A network without any additional constraints and with N_f fibers has $3N_f$ unbound degrees of freedom. Every additional constraint binds one degree of freedom. If we add second-nearest neighbor bonds with some probability p_{sn} , there will be

$$\sum_{r=3}^{\infty} p_{sn} r n_r \quad (3)$$

such constraints. Here n_r is the number of fibers with r crossing points. Hence the number of floppy modes,

$$F = 3N_f - \sum_{r=3}^{\infty} p_{sn} r n_r = 3N_f - p_{sn} \langle r \rangle N_f = 3N_f - 2p_{sn} N_c, \quad (4)$$

where $\langle r \rangle$ is the average number of crossing points on a fiber and N_c is the total number of crossing points in the network.

The number of crossing points is [32]

$$N_c = \frac{(N_f \bar{l})^2}{\pi A}, \quad (5)$$

where \bar{l} is the average length of a fiber. As all the fibers have equal length we can set $\bar{l} = 1$ and as the density of fibers is $q = N_f/A$, where A is the area of the system, we find that

$$N_c = \frac{N_f q}{\pi}. \quad (6)$$

Hence the number of floppy modes per degree of freedom can be expressed in the form

$$f = \frac{F}{2(N_c + 2N_f)} = \frac{3}{\frac{2q}{\pi} + 4} - \frac{1}{\frac{2}{\pi} + 1} p_{sn}, \quad (7)$$

$$p_{sn} \ll p_{sn}^{(c)}.$$

Above the rigidity transition, the behavior of F is dependent on the end nodes since the degrees of freedom associated with these are bound only if there is an snn constraint between the end node and its second-nearest neighbor. The number of these constraints is $2N_f p_{sn}$. As the fiber ends have $2N_f$ unbound degrees of freedom, we get $F = 2N_f - 2N_f p_{sn}$ for $p_{sn} \gg p_{sn}^{(c)}$ and consequently,

$$f = \frac{1}{\frac{q}{\pi} + 2} - \frac{1}{\frac{q}{\pi} + 2} p_{sn}; \quad p_{sn} \gg p_{sn}^{(c)}. \quad (8)$$

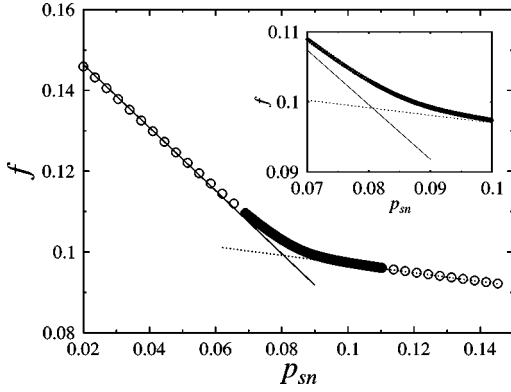


FIG. 3. Number of floppy modes at $q=4q_c$. The solid line is the Maxwell-counting estimate and the dashed line the large p_{sn} estimate. The crossing point of these two linear trends gives a first estimate for the transition point.

The number of floppy modes per degree of freedom, f is plotted in Fig. 3.

Maxwell counting gives a first estimate for the transition point $p_{sn}^{(c)}$. The two trends linear in p_{sn} , Eqs. (7) and (8), cross at $p_{sn} = p_{sn}^{(0)} \approx p_{sn}^{(c)}$,

$$3N_f - 2N_c p_{sn}^{(0)} = 2N_f - 2N_f p_{sn}^{(0)} \quad (9)$$

and thus we find that

$$p_{sn}^{(c)} \approx p_{sn}^{(0)} = \frac{N_f}{2(N_c - N_f)} = \frac{1}{2\left(\frac{q}{\pi} - 1\right)}. \quad (10)$$

This estimate turns out to be increasingly good for increasing (Fig. 4) q . It is evident that this estimate cannot however hold at low densities. If $q < q_c$ ($q_c = 5.71$ being the critical density in connectivity percolation [30]), there cannot exist a rigid percolation cluster since there does not even exist a connected percolation cluster. If, e.g., $q > 3/(2\pi)$, Eq. (9) would imply $p_{sn}^{(c)} < 1$ and we would have a rigid percolation cluster.

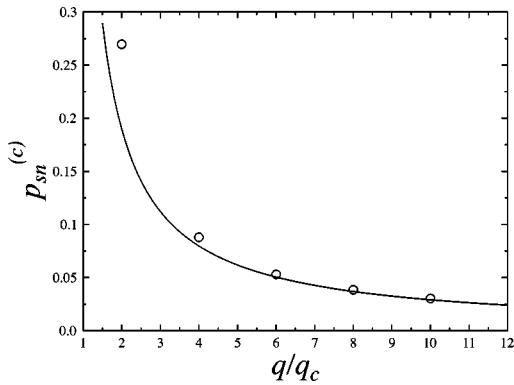


FIG. 4. Comparison of the Maxwell-counting estimate and the actual transition point evaluated numerically. The circles are the transition points and the solid line the Maxwell-counting estimate. The error in the transition points is smaller than the size of the circles.

It is possible to find by Maxwell counting an estimate for $q = q_{min}$ below which there will not exist a rigid percolation cluster. For connectivity, each fiber has one degree of freedom (connected or not) and each crossing point binds one degree of freedom. Hence, at the transition we get

$$N_f = N_c = \frac{N_f q_c}{\pi} \Rightarrow q_c = \pi \quad (11)$$

(more accurately [34], $q_c = 5.71$). This underestimates the critical density because many fibers in the percolation cluster at q_c are multiply connected. For rigidity, each stiff fiber (all snn bonds present) has three degrees of freedom (two translations and a rotation) and each crossing point binds two degrees of freedom,

$$3N_f = 2N_c = \frac{2N_f q_c}{\pi} \Rightarrow q_{min} = \frac{3}{2}\pi. \quad (12)$$

This estimate underestimates q_{min} because it supposes that all constraints are independent and overestimates it because it supposes that all the degrees of freedom need to be bound for a spanning connected network. The estimate $q_{min} = \frac{3}{2}\pi$ is definitely an underestimation because then $q_{min} < q_c$, which is not possible. A next guess would be that $q_{min} = \frac{3}{2}q_c$ because then the estimate for rigidity would fail by the same factor as that for connectivity. At $q = q_{min}$ we would have $p_{sn}^{(c)} = 1$. So for $q = \frac{3}{2}q_c$, $p_{sn}^{(c)}$ should be $p_{sn}^{(c)} = 1$ but Eq. (9) indicates $p_{sn}^{(c)} \approx 0.29$.

B. Characterization of the rigidity transition

It is still unclear under what circumstances rigidity transition is continuous and when it is of first order. In the Cayley tree [18,19,21] and in the square lattice [18,30] with periodic boundary conditions, addition of diagonal bonds leads to a transition, which is of first order. In compact 2D bond (or site) diluted lattices, e.g., the triangular lattice, the transition seems however, to be continuous, and in a different universality class than connectivity-percolation. At low densities (above the connectivity-percolation threshold) the transition is continuous in random networks regardless of the strategy used.

In the limit of infinite density, the random fiber network is statistically similar to the square lattice with a dilute random distribution of diagonal bonds [32], so in this limit the transition could be expected to be of first order. The reason for the similarity of the random fiber network and the square lattice with diagonal bonds is that, at infinite density, their average coordination of nearest neighbors and average coordination of second-nearest neighbors become four (the latter are diluted in both strategies). Although the square lattice with a dilute random distribution of diagonal bonds was shown to have a first-order transition [18], it is unclear what happens in random fiber networks at high but finite densities. We have been able to reach reasonably reliable results for densities $q < 10q_c$. Higher densities are problematic because of the large number of crossing points, e.g., at $q = 20q_c$, a

network of size 100 fiber lengths \times 100 fiber lengths has 41 million crossing points.

When analyzing the nature of a transition, an obvious quantity to check is the free energy, i.e., whether its first derivative is continuous or not. As the free energy associated with the rigidity transition can be taken [14,21] the number of floppy modes in the system. The problem with this approach is that a possible discontinuity only appears for $L \rightarrow \infty$. If the transition is continuous, the number of floppy modes should scale as $f \sim |p - p_c|^{2-\alpha}$, where p is some probability of occupying a lattice, or a density in some appropriate space, so the second derivative of the floppy modes should in this case scale as

$$\frac{d^2 f}{dp^2} \sim |p - p_c|^{-\alpha}. \quad (13)$$

The order parameter will be discontinuous if the transition is of first order. The order parameter [14] is in this case the probability to belong to a rigid percolation cluster. If the transition is continuous, the order parameter will scale as

$$P_\infty \sim (p - p_c)^\beta, \quad p > p_c. \quad (14)$$

In this case of continuous transition, the percolation cluster at the transition threshold will also be statistically self-similar with fractal dimensionality $d_f < 2$. If the transition is of first order, the percolation cluster will scale at the transition threshold with a Euclidian dimension $d = 2$. So for a continuous transition, the mass of the percolation cluster at the transition threshold will scale as

$$M_{p_c}(L) \sim L^{d_f}, \quad d_f < 2. \quad (15)$$

Also the correlation length behaves differently near the transition threshold for a first-order and a continuous transition. In a continuous transition the correlation length ξ diverges at the transition threshold such that

$$\xi \sim |p - p_c|^{-\nu}. \quad (16)$$

C. Correlation length

All the results quoted here are for the *snn* strategy unless otherwise stated. The correlation length gives the typical linear scale within which two mass points belong to the same rigid cluster. It first increases with increasing number of additional constraints as larger and larger parts of the system become constrained. For example, a square consisting of mass points connected with Hooke springs has one floppy motion in which all the four mass points participate. Once a certain threshold is crossed, the redundancy of constraints becomes so high that floppy modes become isolated again and the correlation length begins to decrease. This happens when parts of the system become overconstrained or rigid. On the other hand, one could also consider the size of the typical overconstrained cluster that does not belong to the percolation cluster. The average size of distinct rigid clusters first increases with increasing additional constraints but when the percolation cluster is formed, the individual rigid

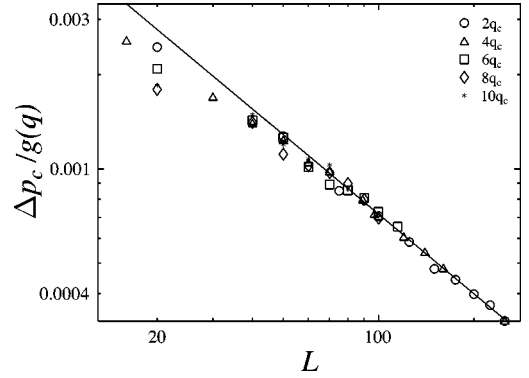


FIG. 5. Determination of the ν exponent from Δp_c . The fitted curve is $0.03L^{-0.84 \pm 0.02}$.

clusters merge with the percolation cluster as additional constraints are added to the network.

We use here an indirect way to determine the correlation-length exponent ν . If the probability of finding a percolation cluster at a probability p of additional constraints is considered, the correlation-length exponent can be found in two ways. First, the highest value of the first derivative of this probability scales as $L^{-\nu}$. On the other hand, the standard deviation of the critical probability at which there exists a percolation cluster in a system of linear size L scales as $L^{-1/\nu}$ [1]. Furthermore, by taking into account the effect of density q , one finds that

$$\begin{aligned} \Delta p_c(L, p - p_c, q) &= L^{-1/\nu} f[(p - p_c)^\nu L] g(q) \\ &= f(0) L^{-1/\nu} g(q). \end{aligned} \quad (17)$$

Here f and g are some functions. From our numerical results for $\Delta p_c(L, p - p_c, q)$ with the *snn* strategy, we find that $\nu = 1.19 \pm 0.03$ (Fig. 5).

By considering the probability $\pi(p, L)$ of finding a rigid percolation cluster at probability p of additional constraints in a system of size $L \times L$, we can accurately determine the transition probability p_c . Plotting the probability p_x at which $\pi(p_x, L) = x$ as a function of $L^{-1/\nu}$, we get a set of lines that cross at $L = \infty$, and the crossing point defines the transition probability p_c . This kind of scaling also gives a possibility to determine the correlation-length exponent with data collapse,

$$\pi(p - p_c, L) = L^{-1/\nu} \phi[(p - p_c)^\nu L]. \quad (18)$$

Here $\phi(x)$ is again some (scaling) function.

There is also another way to independently determine the correlation-length exponent by using the number of cutting bonds as this number should scale as $L^{1/\nu}$ [13]. For a given network, we have used 200–2000 different realizations of the additional constraints and for a given size and density we have used 10–100 different networks. We have used sizes of 20–250 fiber lengths with densities of 2–10 times the percolation density. A scaling analysis (Fig. 6) gave $\nu = 1.20 \pm 0.03$ for all bonds and $\nu = 1.19 \pm 0.03$ for the *snn* bonds.

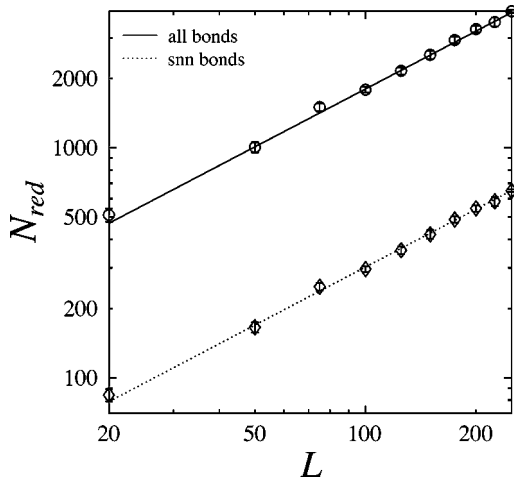


FIG. 6. Scaling of the number of cutting bonds N_{red} . Circles denote the numerical results for all bonds and diamonds for the *snn* bonds. The solid line is $3.65L^{0.83 \pm 0.02}$ and the dashed line $1.86L^{0.837 \pm 0.015}$.

D. Order parameter and the structure of percolation cluster

Below the transition threshold there is no rigid cluster that would span across the system. It only appears above the transition. At exactly the transition threshold, the rigid percolation cluster is fractal, i.e., it scales as L^{D_f} with $D_f < 2$ if the transition is continuous. This means that for $L \rightarrow \infty$ the density of the rigid percolation cluster becomes infinitesimal.

So for a continuous transition, the order parameter is zero below the transition and goes continuously to zero at the transition threshold when $L \rightarrow \infty$.

Consider next the behavior of the order parameter near the transition threshold. Periodic boundary conditions are used in the y direction and the left and right boundaries of the network are connected to rigid bars. We then place an additional fictitious bond between the two rigid bars and monitor when this bond becomes redundant. When the fictitious bond is recognized as redundant, there is a rigid stress-bearing backbone in the network that was formed at the last step. The bonds that are recognized as redundant only at the last step are called the cutting bonds. Not one of the cutting bonds can be removed without losing the rigid stress-bearing backbone. Once the backbone is recorded, we record the isostatic, i.e., minimally rigid areas of the network. These areas are rigidly connected to the backbone but do not carry stress. The recording of the isostatic areas is performed by checking whether a crossing point, which is not in the backbone, is rigidly connected to the backbone. This is done by adding a fictitious bond between the crossing point and one of the crossing points in the rigid backbone. A rigid percolation cluster is shown in Fig. 7.

For a given network we have used 200–2000 different realizations of the additional constraints, and for a given size and density 10–100 different realizations of the network. Networks of linear sizes of 20–250 fiber lengths were used when determining the backbone, and of 16–100 fiber lengths

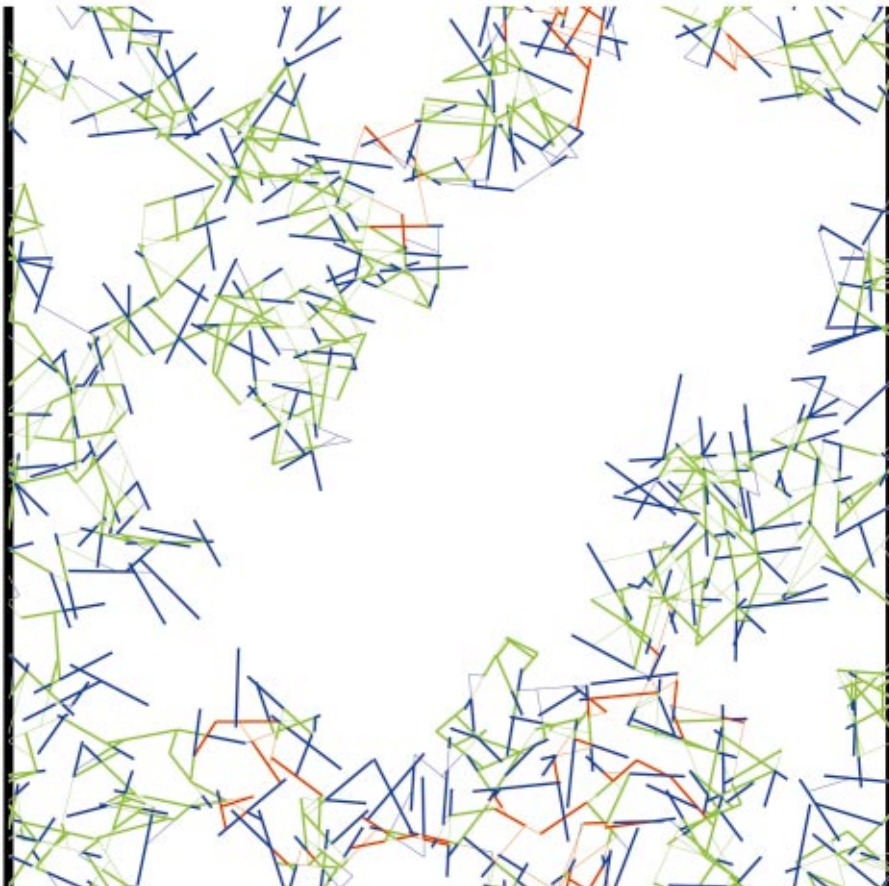


FIG. 7. (Color) A percolation cluster at the transition point. Red bonds denote the cutting bonds, green bonds the rigid backbone, and blue bonds the isostatic areas.

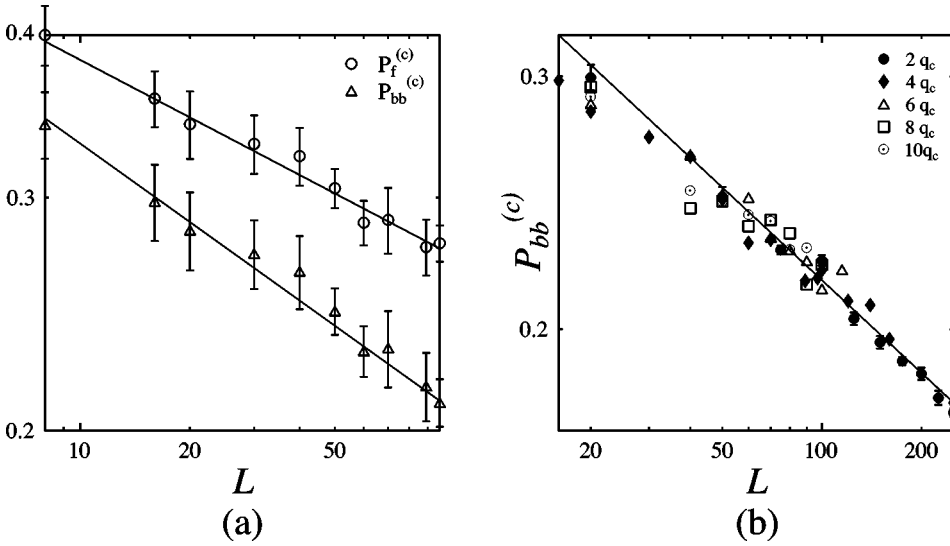


FIG. 8. (a) Probability of belonging to the percolation cluster at $q=4q_c$, $P_f^{(c)}$ and probability to belong to the backbone $P_{bb}^{(c)}$. These data give $d_f=1.85\pm 0.3$ and $d_{bb}=1.80\pm 0.03$. (b) Probability of belonging to the backbone for $2q_c \leq q \leq 10q_c$. These data give $d_{bb}=1.79\pm 0.03$.

when determining the isostatic areas, while the densities varied in the range 2–10 times the critical density of connectivity percolation. At p_{sn}^{crit} the number of bonds in the backbone, the number of cutting bonds, and the number of bonds in the isostatic parts of the network were recorded. From these the fractal dimension of the backbone and the fractal dimension of the rigid percolation cluster were determined by log-log least-squares fits. In Fig. 8(a) the probabilities of belonging to the fractal cluster (P_f) and to the backbone (P_{bb}) are plotted at $p=p_{sn}^{crit}$ as functions of network size L for $q=4q_c$. As the number of bonds in fractal cluster (backbone) scales as $N_f \sim L^{d_f}$ ($N_{bb} \sim L^{d_{bb}}$) and the total number of bonds scales as $N \sim L^2$, these probabilities will scale as

$$P_f = \frac{N_f}{N} \sim L^{d_f-2} (P_{bb} \sim L^{d_{bb}-2}) \quad (19)$$

when $L \rightarrow \infty$. We find $P_f = 0.53L^{0.15 \pm 0.03}$, which gives $d_f = 1.85 \pm 0.03$.

In Fig. 8(b) the probability of belonging to the backbone is plotted as a function of L for densities $2q_c \leq q \leq 10q_c$. The curve in this figure is a linear fit to the numerical points for sizes $L \geq 40$. This gives $P_{bb} = 0.58L^{0.21 \pm 0.03}$ and $d_{bb} = 1.79 \pm 0.03$. The errors are estimated from linear fits to all combinations of three or more points through the standard deviations of the slopes. It is evident that the backbone appears to be fractal but the asymptotic behavior could not be reached by going to larger system sizes mainly because of difficulties with the determination of the isostatic bonds.

As the transition threshold is crossed by adding constraints, the number of bonds in the backbone and the number of bonds in the rigid percolation cluster are monitored. Thereby the order parameter can be evaluated both for the backbone and for the rigid percolation cluster. For the rigid percolation cluster only the network size of 20×20 fiber lengths was used as the determination of the isostatic areas because this calculation is time consuming. For the backbone, we used linear network sizes of 20–60 fiber lengths. For these sizes, finding the scaling regime (between the finite-size-dominated behavior and the constant behavior) is

always tricky. It was, however, possible to evaluate with some accuracy the scaling regime. Close to the transition point, the order parameter is a convex function of $p-p_c$, i.e., in a log-log plot the (local) slope of the order parameter is close to or larger than 1. Away from the transition, the order parameter (probability to belong to the rigid cluster) tends to a constant (zero slope). Hence there are crossovers from convex to scaling behavior to a constant behavior, which usually makes it difficult to find the scaling regime. Considering instead the probability of an *snn* bond to belong to the percolation cluster (or the backbone), makes the scaling regime easier to detect. Now the crossovers are from convex to scaling to linear since $\beta, \beta_{bb} < 1$. This means that we should look (in log-log plots) for an intermediate linear regime in the slope. This linear regime becomes, as expected, larger with increasing system size. We have used the average of p_{sn}^{crit} and the point of the largest slope of the order parameter to evaluate the p_c . Both seem to give the same β exponent.

We have evaluated the β exponent using finite-size scaling of the order parameter at the average transition point and also by straightforward fits by $P_\infty \sim (p-p_c)^\beta$. The latter method gives $\beta = 0.18 \pm 0.02$ and $\beta_{bb} = 0.23 \pm 0.02$. The errors are determined from fits to each network realization by standard deviation of the fitted exponents. In Fig. 9(a) the probability of an *snn* bond belonging to the rigid percolation cluster is plotted for 10 network realizations of size 20×20 fiber lengths at $q=4q_c$. The scaling regime is apparent although quite short. The scaling function $f(z)$ for β_{bb} is determined by

$$\begin{aligned} P_{bb^\infty}(p-p_c, L) &= L^{-\beta/\nu} P_{bb^\infty}((p-p_c)L^{1/\nu}, 1) \\ &= L^{-\beta/\nu} f((p-p_c)L^{1/\nu}). \end{aligned} \quad (20)$$

In Fig. 9(b) we use data collapse to show scaling for the *snn* bonds in the backbone. Here we used $\nu = 1.19$. The best data collapse was found for $\beta_{bb} = 0.24$ while the scaling function has a slope of $\beta_{bb} = 0.23$ in the log-log plot.

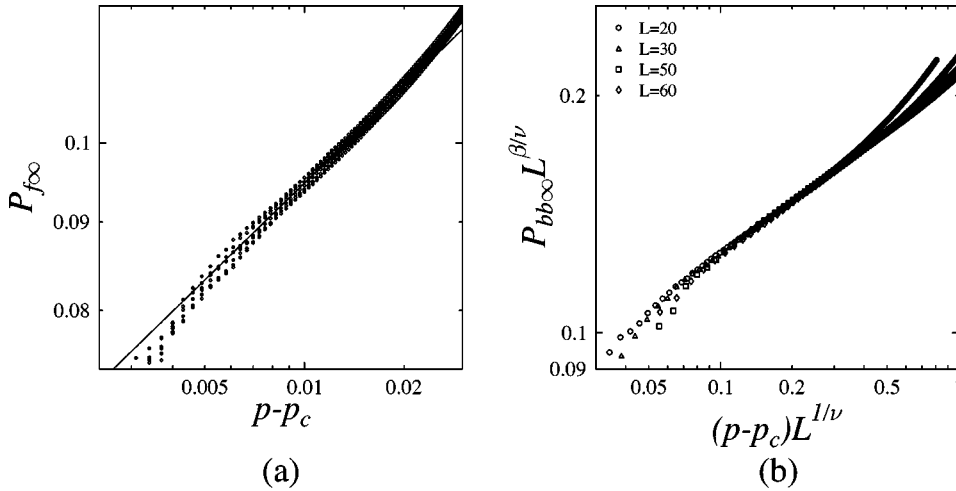


FIG. 9. (a) Probability of belonging to the percolation cluster at $q=4q_c$ as a function of $(p-p_c)$, i.e., the order parameter and (b) data collapse of P_{bb} . The slope of the intermediate linear regime is quite robust and does not depend much on the p_c used, only the position of this regime changes as p_c is changed.

E. Number of floppy modes

In the connectivity percolation the quantity that behaves like the free energy is the number of clusters. The number of clusters is an extensive quantity and has the right convexity properties, i.e., its second derivative with respect to probability p to occupy a site or bond is positive for all p . In the rigidity percolation the number of rigid clusters does not have the right convexity properties and thus cannot be chosen as the free energy. Instead, the number of floppy modes does have [12,14] the required properties.

The number of floppy modes is a measure of independent motions in the network that do not cost energy. We are now interested in what happens to df/dp at the rigidity transition as $L \rightarrow \infty$. Using the pebble game [12] it is straightforward to calculate the number of floppy modes for a given network and for a given distribution of additional constraints. In Fig. 10 the first and the second derivatives of the number of floppy modes are plotted.

For all the fiber networks we have used 1000 different realizations of the additional constraints, and for a given size and density we have used 10–500 different realizations of the fiber network. The linear sizes used have been 4–100 fiber lengths and the densities 2–10 times the critical density of connectivity percolation. As the transition threshold is crossed, the number of floppy modes and the probability that the new constraint is on an already rigid area (effectively the first derivative of the number of floppy modes) are recorded. These are then averaged over all the networks for the transi-

tion threshold (i.e., the point of largest first derivative of the number of floppy modes). There are also more effective ways of finding the transition point. These are already discussed in the earlier sections above. The exponent α was estimated by fitting to the data the function

$$\frac{df}{dp} = \begin{cases} \Gamma_+(p-p_c)^{1-\alpha} + A(p-p_c) + B, & p \geq p_c \\ \Gamma_-(p-p_c)^{1-\alpha} + A(p-p_c) + B, & p < p_c. \end{cases} \quad (21)$$

We found that $\alpha \approx 0.5$, which has been found for central-force rigidity percolation in diluted lattices [12], is not in violation with the data.

IV. CONCLUSIONS

Rigidity percolation in 2D random networks can be effectively studied using matching algorithms [11–13]. The transition from floppy to rigid is quite narrow, which means that below the transition, the number of floppy modes is well approximated by Maxwell counting. The Maxwell-counting estimate for the transition point becomes increasingly accurate as the density of the network is increased. The matching algorithm [11,12] gives an accurate way to numerically estimate the transition point.

The rigid backbone of the network is fractal at the transition point. The rigid percolation cluster also appears fractal, and the order parameter and the first derivative of the free energy are continuous, which means that there is a continu-

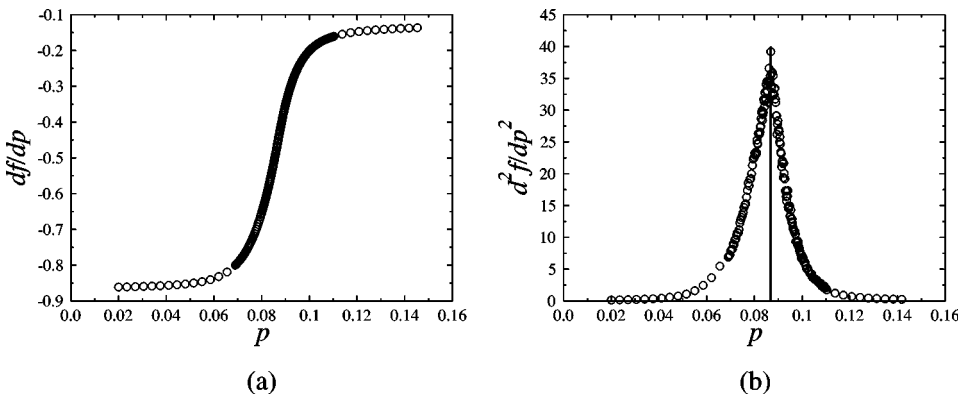


FIG. 10. (a) The first derivative of the number of floppy modes and (b) the second derivative of the number of floppy modes; the solid line denotes the estimate for the transition probability $p_{sn}^{(c)}$.

ous transition from floppy to rigid. From our numerical results we have evaluated that $\nu=1.19\pm 0.03$, $\beta=0.18\pm 0.02$, $\beta_{bb}=0.23\pm 0.02$, $d_f=1.85\pm 0.03$, and $d_{bb}=1.79\pm 0.03$. Of these exponents, ν and d_{bb} were both evaluated for the *snn* bond and the welding constraints; all others are for the *snn*-bond constraints alone. Regardless of the rigidifying strategy, the estimates for the critical exponents suggest that the transition belongs to the universality class of the 2D lattice-diluted central-force rigidity percolation. We expect to have determined the transition points very accurately and the exponents ν and d_{bb} with a reliable accuracy. Other exponents satisfy the scaling relations with a fair accuracy, so we also are confident about the estimates for these exponents. At high densities it is still not quite clear whether the transition is continuous or not. It seems to be possible to derive eventually some analytic results in the limit $q\rightarrow\infty$. At $q=\infty$ the average coordination number of the network is 4, and the *snn* bonds play a similar role as the diagonal bonds in square lattices, so the transition might be expected to be of first order.

The main limiting factor in using the pebble game is the amount of memory required to keep track of the pebble game and the network topology. We have been able to handle 11 000 000 nodes or crossing points. This means a size of 250×250 fiber lengths for a density of four times that of the connectivity-percolation threshold. The estimation of the correlation-length exponent ν and the order-parameter exponent β could be done quite reliably. Similarly, the fractal dimensions could be obtained with a relatively good accuracy. The problematic exponent was the specific-heat exponent α . Since there are five fitting parameters (Γ, p_c, α, A , and B), the fits were fairly arbitrary. All that could be said is that $\alpha\approx 0.5$, which is the exponent for 2D central-force rigidity percolation, is not in violation with the data. For the sizes of 4–100 fiber lengths, the scaling regime for the α exponent was quite narrow. Once $p\rightarrow p_c$, i.e., $\xi>L$, we

could only see the linear trend. For $|p-p_c|$ large, we could only see the $df/dp=\text{const}$ regime. There must, of course, be a crossover from linear to scaling behavior to a constant, and these crossovers further complicate the finding of the scaling regime. Fitting of the free energy would require one more fitting parameter and hence would make the fits even more arbitrary. One might think that one should fit instead the second derivative but the problem there is that if the second derivative is calculated numerically, it is far too coarse to be fitted sensibly by any function. If one would use a Monte Carlo method to find the second derivative directly, it would increase dramatically the calculation time required.

We have demonstrated that at least for low densities and with additional constraints as the driving parameters, the rigidity transition in 2D random fiber networks, with the segments between the crossing points considered as Hooke springs, is in the universality class of the 2D central-force rigidity percolation. The future work could be associated with the low-density and high-density limits. With the low-density limit we mean the case that the fibers itself are absolutely rigid and the density is the driving parameter. For high densities, it is plausible that this problem can eventually be mapped to the diagonal-bond square-lattice problem already solved.

ACKNOWLEDGMENTS

We would like to thank Michael Thorpe for his interesting suggestions and for the Jacobs-Thorpe ‘‘pebble game’’ code. We would also like to thank Cristian Moukarzel for fruitful discussions. The contribution to this work by Markku Kellomäki is also acknowledged. This work has been supported by the Academy of Finland under the Finnish Center of Excellence Programme 2000-2005 (Project No. 44875, Nuclear and Condensed Matter Programme at JYFL) and under the Matra Programme (Project No. 16498).

-
- [1] D. Stauffer and A. Aharony, *Introduction to Percolation Theory*, 2nd ed. (Taylor & Francis, London, 1994).
 - [2] See, e.g., M. B. Isichenko, *Rev. Mod. Phys.* **64**, 961 (1992) for a review containing 2D and 3D connectivity-percolation exponents with an extensive list of references; M. P. M. den Nijs, *J. Phys. A* **12**, 1857 (1979); R. B. Pearson, *Phys. Rev. B* **22**, 2579 (1980); B. Nienhuis, *Phys. Rev. Lett.* **49**, 1062 (1982) for exact evaluation of the independent geometrical exponents.
 - [3] S. Feng and P. Sen, *Phys. Rev. Lett.* **52**, 216 (1984).
 - [4] Y. Kantor and I. Webman, *Phys. Rev. Lett.* **52**, 1891 (1984).
 - [5] S. Feng, P. Sen, B. Halperin, and C. Lobb, *Phys. Rev. B* **30**, 5386 (1984).
 - [6] A. R. Day, R. R. Tremblay, and A.-M. S. Tremblay, *Phys. Rev. Lett.* **56**, 2501 (1986).
 - [7] S. Roux and A. Hansen, *Europhys. Lett.* **6**, 301 (1988).
 - [8] A. Hansen and S. Roux, *Phys. Rev. B* **40**, 749 (1989).
 - [9] S. Arbabi and M. Sahimi, *Phys. Rev. B* **47**, 695 (1993).
 - [10] S. P. Obukhov, *Phys. Rev. Lett.* **74**, 4472 (1995).
 - [11] B. Hendrickson, *SIAM J. Comput.* **21**, 65 (1992).
 - [12] D. J. Jacobs and M. F. Thorpe, *Phys. Rev. Lett.* **75**, 4051 (1995).
 - [13] C. Moukarzel and P. M. Duxbury, *Phys. Rev. Lett.* **75**, 4055 (1995).
 - [14] D. J. Jacobs and M. F. Thorpe, *Phys. Rev. E* **53**, 3682 (1996).
 - [15] C. Moukarzel, *J. Phys. A* **29**, 8079 (1996).
 - [16] D. J. Jacobs and B. Hendrickson, *J. Comput. Phys.* **137**, 346 (1997).
 - [17] M. Kellomäki, J. Åström, and J. Timonen, *Phys. Rev. Lett.* **77**, 2730 (1996).
 - [18] C. Moukarzel, P. M. Duxbury, and P. L. Leath, *Phys. Rev. Lett.* **78**, 1480 (1997).
 - [19] C. Moukarzel, P. M. Duxbury, and P. L. Leath, *Phys. Rev. E* **55**, 5800 (1997).
 - [20] A. Losev and F. Babalievski, *Physica A* **252**, 1 (1998).
 - [21] P. M. Duxbury, D. J. Jacobs, M. F. Thorpe, and C. Moukarzel, *Phys. Rev. E* **59**, 2084 (1999).
 - [22] W. Tang and M. F. Thorpe, *Phys. Rev. B* **37**, 5539 (1988).
 - [23] S. J. Barsky, M. Plischke, B. Joós, and Z. Zhou, *Phys. Rev. E* **54**, 5370 (1996).

- [24] D. H. Boal, Phys. Rev. E **47**, 4604 (1993).
- [25] W. Bresser, P. Boolchand, and P. Suranyi, Phys. Rev. Lett. **56**, 2493 (1986).
- [26] Y. Cai and M. F. Thorpe, Phys. Rev. B **40**, 10 535 (1989).
- [27] P. Boolchand and M. F. Thorpe, Phys. Rev. B **50**, 10 366 (1994).
- [28] S. S. Yun, H. Lin, R. L. Cappalletti, R. N.ENZWEILER, and P. Boolchand, Phys. Rev. B **39**, 8702 (1989).
- [29] R. Aravinda Narayanan and A. Kumar, Phys. Rev. B **60**, 11 859 (1999).
- [30] C. Moukarzel and P. M. Duxbury, Phys. Rev. E **59**, 2614 (1999).
- [31] M. A. de Menezes and C. Moukarzel, Phys. Rev. E **60**, 5699 (1999).
- [32] O. Kallmes and H. Korte, Tappi J. **43**, 737 (1960).
- [33] J. C. Maxwell, Philos. Mag. **27**, 294 (1864).
- [34] G. E. Pike and C. H. Seager, Phys. Rev. B **10**, 1421 (1974).